

Type-Based Unsourced Multiple Access

Khac-Hoang Ngo, Deekshith Pathayappilly Krishnan, Kaan Okumus, Giuseppe Durisi, and Erik G. Ström
Department of Electrical Engineering, Chalmers University of Technology, 41296 Gothenburg, Sweden

Abstract—We generalize the type-based multiple access framework proposed by Mergen and Tong (2006) to the case of unsourced multiple access. In the proposed framework, each device tracks the state of a physical/digital process, quantizes this state, and communicates it to a common receiver through a shared channel in an uncoordinated manner. The receiver aims to estimate the type of the states, i.e., the set of states and their multiplicity in the sequence of states reported by all devices. We measure the type estimation error using the Wasserstein distance. Considering an example of multi-target position tracking, we show that type estimation can be performed effectively via approximate message passing. Furthermore, we determine the quantization resolution that minimizes the type estimation error by balancing quantization distortion and communication error.

I. INTRODUCTION

Future Internet of Things (IoT) services are enabled by the capability to collect data from a massive number of low-cost distributed devices.¹ These devices transmit short packets in a sporadic and uncoordinated manner. To address this scenario, Polyanskiy proposed the unsourced multiple access (UMA) framework [1], where all users employ a common codebook and the receiver returns an unordered list of messages. This work ignited an active research area that aims to characterize theoretical limits on the achievable energy efficiency [2], [3] and devise coding schemes approaching these limits [4], [5].

In UMA, the users generate their messages independently and the receiver treats any message collision between users as an error. However, real-world scenarios often involve messages describing physical/digital processes correlated across users. Moreover, the receiver may be interested not only in the set of transmitted messages but also in their frequency of occurrence. For instance, in multi-target tracking [6]–[8], each message may represent the state of a target, and the receiver may seek to estimate the number of sensors tracking each target. In federated learning, each message may correspond to a quantized local model update. To aggregate these updates, the server needs to estimate the number of users submitting each quantized update [9], [10]. In these contexts, the users *sense/sample* parameters from physical/digital processes, *quantize* these parameters, and *communicate* them to the receiver. The UMA framework focuses only on the communication phase.

The problem of estimating the type, i.e., the number of users sending each message, was formulated in [11] under the name of type-based multiple access (TBMA). However, the authors assume that each message is assigned an orthogonal codeword, which entails a large latency if the number of messages is large. Recent research has explored type estimation in random-access scenarios with nonorthogonal codewords. In particular, [12] considers IoT monitoring over a fog radio access network, [13] proposes an information-bottleneck-based

codebook design and a neural-network-based decoder, and [9] addresses the federated learning setup. However, these works consider small systems [12], [13]. Hence, it is unclear whether the proposed solutions can be applied to the massive access regime. Moreover, they consider a specific application [9], [13] rather than developing a general framework.

In this paper, we present type-based unsourced multiple access (TUMA), a setup that bridges TBMA and UMA, propose a general performance metric for this setup, and benchmark under this metric three algorithms to estimate the type. In our framework, we assume that a large number of users track the states of multiple processes and report these states to a receiver. Each user tracks a process and represents the state of this process by a message that is used to i) map the state to a quantized state belonging to a quantization codebook, and ii) select an element of a communication codebook. Both the quantization and communication codebooks are the same for all users. To report the state, the user sends the corresponding communication codeword in an uncoordinated manner. The receiver aims to estimate the type of the states, i.e., the set of distinct states and their multiplicity in the sequence of states reported by all users. To assess the type estimation error, we use the Wasserstein distance, a metric commonly used in optimal transport [14].

We compare three existing type estimators: the approximate message passing (AMP) estimator derived for UMA in [4], the scalar AMP estimator derived in [15, Sec. IV-C] and adopted in [9], and the expectation propagation (EP) estimator derived in [15, Sec. IV-D]. The AMP estimator turns out to have the same complexity order as scalar AMP and a lower complexity order than EP. Via an example pertaining to multi-target position tracking, we show that AMP also achieves a better performance than scalar AMP and EP. Our numerical results highlight a trade-off between quantization and communication: increasing the quantization resolution reduces the distortion but degrades the communication performance. The average Wasserstein distance is minimized at a certain quantization resolution. Remarkably, the optimal resolution cannot be achieved using orthogonal codebooks as in TBMA [11].

Notation: We denote system parameters by uppercase non-italic letters, e.g., K . Uppercase italic letters, e.g., X , denote scalar random variables and their realizations are written in lowercase, e.g., x . Vectors are denoted likewise with boldface letters, e.g., a random vector \mathbf{X} and its realization \mathbf{x} . We denote the $n \times n$ identity matrix by \mathbf{I}_n . The superscript T stands for transposition. We denote sets with calligraphic letters, e.g., \mathcal{S} , the Gaussian vector distribution with mean $\boldsymbol{\mu}$ and covariance matrix \mathbf{A} by $\mathcal{N}(\boldsymbol{\mu}, \mathbf{A})$, and its

¹In this paper, we shall refer to devices also as users or sensors.

probability density function (PDF) by $\mathcal{N}(\cdot; \boldsymbol{\mu}, \mathbf{A})$. We denote the probability mass function (PMF) of a binomial distribution with parameters (n, p) by $\text{Bin}(\cdot; n, p)$. We use $\|\cdot\|$ to denote the ℓ^2 -norm; $[n] = \{1, \dots, n\}$; \propto means ‘‘proportional to’’. We define a discrete measure with weights p_1, \dots, p_n (with $\sum_{i=1}^n p_i = 1$) and locations $\mathbf{x}_1, \dots, \mathbf{x}_n \in \mathcal{X}$ as $\sum_{i=1}^n p_i \delta(\mathbf{x}_i)$, where $\delta(\cdot)$ is the Dirac measure. The set of all discrete measures defined on \mathcal{X} is denoted by $\mathcal{P}(\mathcal{X})$.

Reproducible Research: The Matlab code used to generate our numerical results is available at: <https://github.com/khachoang1412/TUMA>.

II. SYSTEM MODEL

We consider a setting in which a large number of sensors track the states of M_a targets and report these states, in an coordinated way, to a receiver over N uses of a stationary Gaussian multiple access channel. At a given time, K_a sensors are active, i.e., they see a target. In a typical IoT setting, K_a , M_a , and N are in the order of 10^2 – 10^3 , 10^1 – 10^2 , and 10^3 – 10^4 , respectively—see [1] and [16, Rem. 3]. For concreteness, we will focus on a multi-target tracking scenario and use terms such as ‘‘sensors’’, ‘‘targets’’, and ‘‘states’’. However, as we shall clarify at the end of this section, the setup is general. Let $\mathbf{X}_k \in \mathbb{R}^N$ be the signal transmitted by sensor k . The corresponding received signal is given by

$$\mathbf{Y} = \sum_{k=1}^{K_a} \mathbf{X}_k + \mathbf{Z} \quad (1)$$

where $\mathbf{Z} \sim \mathcal{N}(\mathbf{0}, \mathbf{I}_N)$ is the Gaussian noise, which is independent of the transmitted signals. The transmitted signals satisfy the power constraint $\|\mathbf{X}_k\|^2 \leq NP$, $\forall k \in [K_a]$. Here, P is also identified with the signal-to-noise ratio (SNR).

We now describe how the transmitted signals are generated. Each target $i \in [M_a]$ has a state \mathbf{S}_i (e.g., its position) generated from a state space \mathcal{S} according to a distribution $p_{\mathcal{S}}$. We assume that each sensor k reports the state of a single target O_k , and that this target is selected according to a distribution p_{O_k} . Specifically, we assume that the sensor maps \mathbf{S}_{O_k} to one of the quantized states in a quantization codebook $\mathcal{Q} = \{\mathbf{q}_1, \dots, \mathbf{q}_M\}$. Let $W_k \in [M]$ be the index of the quantized state associated to \mathbf{S}_{O_k} . To report W_k to the receiver, sensor k transmits $\mathbf{X}_k = \sqrt{NP} \mathbf{c}_{W_k}$ where \mathbf{c}_{W_k} belongs to a communication codebook $\mathcal{C} = \{\mathbf{c}_1, \dots, \mathbf{c}_M\}$ with $\|\mathbf{c}_i\| \leq 1$, $\forall i \in [M]$. All sensors employ the same quantization codebook \mathcal{Q} and communication codebook \mathcal{C} . The receiver aims to estimate the discrete measure $\sum_{i=1}^{M_a} T_i \delta(\mathbf{S}_i)$, where $T_i \in [0, 1]$ is the fraction of sensors that report target $i \in [M_a]$, i.e., the number of sensors reporting target i is $T_i K_a$. This measure represents the type of the sequence $\mathbf{S}_{O_1}, \dots, \mathbf{S}_{O_{K_a}}$.

For a given quantization codebook \mathcal{Q} and communication codebook \mathcal{C} , the design of a TUMA system consists of specifying the following functions:²

²We assume perfect sensing, i.e., the sensors know the exact state of their tracked target. Sensing errors can be straightforwardly incorporated in our model by introducing a sensing function before the quantization function.

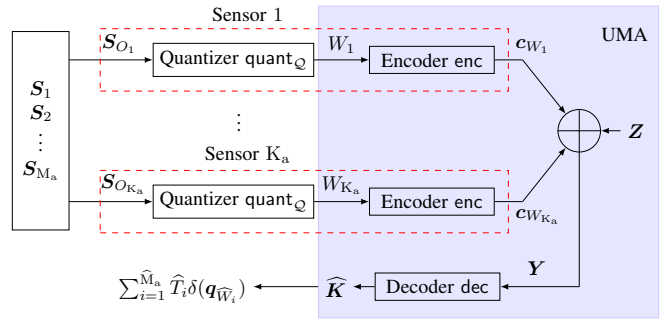


Fig. 1. Illustration of the proposed TUMA framework and its relation to UMA, which is represented by the shaded box.

- A quantization function $\text{quant}_{\mathcal{Q}} : \mathcal{S} \rightarrow [M]$ that produces the message $W_k = \text{quant}_{\mathcal{Q}}(\mathbf{S}_{O_k})$ of sensor k associated to the state \mathbf{S}_{O_k} of the target O_k tracked by sensor k . The quantized state of target O_k is then \mathbf{q}_{W_k} .
- An encoding function $\text{enc} : [M] \rightarrow \mathcal{C}$ that produces the codeword $\mathbf{c}_{W_k} = \text{enc}(W_k)$ corresponding to the message W_k .
- A decoding function $\text{dec} : \mathbb{R}^N \rightarrow \mathcal{P}(\mathcal{Q})$ that provides an estimate of $\sum_{i=1}^{M_a} T_i \delta(\mathbf{S}_i)$. Specifically, the decoder first finds an estimate $\hat{\mathbf{K}} = [\hat{K}_1, \dots, \hat{K}_M]^T$ of $\mathbf{K} = [K_1, \dots, K_M]^T$, where K_i is the number of sensors that send message $i \in [M]$. Then, it estimates the type as $\sum_{i=1}^M \frac{\hat{K}_i}{\sum_{j=1}^M \hat{K}_j} \delta(\mathbf{q}_i)$. The estimated type can be written compactly as $\sum_{i=1}^{\hat{M}_a} \hat{T}_i \delta(\mathbf{q}_{\hat{W}_i})$ where $\hat{M}_a = |\{i \in [M] : \hat{K}_i > 0\}|$, $\{\hat{W}_1, \dots, \hat{W}_{\hat{M}_a}\} = \{i \in [M] : \hat{K}_i > 0\}$, and $\hat{T}_i = \hat{K}_{\hat{W}_i} / \sum_{j=1}^M \hat{K}_j$, $i \in [\hat{M}_a]$. Hereafter, we assume that the number of targets M_a and the number of sensors K_a are known to the decoder. Note that since some targets may not be tracked by any sensor and multiple targets may be mapped to a common quantized state, we may have that $|\{i \in [M] : K_i > 0\}| < M_a$. Therefore, the decoder may return a type with support size $\hat{M}_a < M_a$.

To assess the type estimation error, we consider the metric

$$\overline{\mathbb{W}}_p = \mathbb{E} \left[\mathbb{W}_p \left(\sum_{i=1}^{M_a} T_i \delta(\mathbf{S}_i), \sum_{i=1}^{\hat{M}_a} \hat{T}_i \delta(\mathbf{q}_{\hat{W}_i}) \right) \right] \quad (2)$$

where the expectation is with respect to $p_{\mathcal{S}}$, $\{p_{O_k}\}_{k=1}^{K_a}$, and the additive noise. Here, $\mathbb{W}_p(\cdot, \cdot)$ is the p -Wasserstein distance [14, Chap. 2] defined as

$$\begin{aligned} & \mathbb{W}_p \left(\sum_{i=1}^{M_a} T_i \delta(\mathbf{S}_i), \sum_{i=1}^{\hat{M}_a} \hat{T}_i \delta(\mathbf{q}_{\hat{W}_i}) \right) \\ &= \inf_{e_{i,j} \in [0,1], i \in [M_a], j \in [\hat{M}_a]} \left(\sum_{i=1}^{M_a} \sum_{j=1}^{\hat{M}_a} e_{i,j} \|\mathbf{S}_i - \mathbf{q}_{\hat{W}_j}\|^p \right)^{1/p} \quad (3) \\ & \text{subject to } \sum_{i=1}^{M_a} e_{i,j} = \hat{T}_j, \sum_{j=1}^{\hat{M}_a} e_{i,j} = T_i. \end{aligned}$$

The Wasserstein distance provides a measure of similarity between distributions that captures both their shape and support. This distance and its generalizations have been widely used in multi-target tracking [6]–[8].

We illustrate the proposed TUMA framework in Fig. 1. This framework generalizes both UMA [1] and TBMA [11]. We highlight next some key differences. First, UMA accounts for

the transmission of the messages $\{W_k\}_{k=1}^{K_a}$ and the support recovery of this set. That is, an UMA system consists only of the encoder and decoder in Fig. 1. In TUMA, we let these messages represent the quantized states of the targets and aim to recover the type of the reported states. Second, in UMA, the messages $\{W_k\}_{k=1}^{K_a}$ are generated uniformly at random from $[M]$, and because $K_a \ll M$, the messages are likely distinct. UMA treats message repetitions as errors. In TUMA, we regard such repetitions as a component of the type to be estimated by the receiver. UMA addresses the per-sensor communication error: an error occurs for sensor k if $W_k \notin \{\widehat{W}_i\}_{i=1}^{M_a}$. In TUMA, we address the overall type-estimation performance. Finally, while the original TBMA framework [11] assumes that $N \geq M$ and thus \mathcal{C} contains orthogonal codewords, TUMA allows N to be smaller than M , a scenario for which orthogonal codewords are not possible.

The TUMA framework is relevant not only for multi-target tracking but also for various other scenarios, including the following.

1) *IoT Monitoring System*: K_a IoT sensors monitor the status of a system and send updates to a gateway. Let the M_a targets be M_a events that occur at a given time and trigger the sensors. Each event is identified by its index out of M possible events, and can be reported by multiple sensors. The common-alarm scenario considered in [17] is a special case of this setup. It corresponds to the case in which only one event occurs and is reported by all sensors.

2) *Point-Cloud Transmission* [18]: A point cloud is a collection of three-dimensional (3D) data points and their associated attributes (such as color and temperature) generated by, e.g., light detection and ranging (LiDAR) sensors and depth cameras. To represent the 3D points, we let the state space \mathcal{S} be a 3D volume. The quantization codebook defines a regular 3D grid. Each state corresponds to a point in the grid. Different LiDAR sensors/cameras detect different points based on their angle of view, and report these points to the receiver.

3) *Digital Over-the-Air Computation* [9]: In this scenario, the sensors coincide with the targets and correspond to clients in a distributed system. The states correspond to local vectors at the clients. The clients submit their vectors to a central server which computes the mean of these vectors. This is a subroutine in many distributed learning and optimization schemes, such as federated learning. Following TUMA, each client quantizes its vector and sends the quantization index to the server. The server estimates the type of the vectors submitted by all clients and computes the mean of the estimated type.

III. DECODER DESIGN

In this section, we discuss the design of decoding function dec. We rewrite the received signal (1) as

$$\mathbf{Y} = \sqrt{NP} \sum_{i=1}^M K_i \mathbf{c}_i + \mathbf{Z} = \sqrt{NP} \mathbf{C} \mathbf{K} + \mathbf{Z}, \quad (4)$$

where $\mathbf{C} = [\mathbf{c}_1, \dots, \mathbf{c}_M]$ is the codebook matrix. Given a realization \mathbf{y} of \mathbf{Y} , we aim to estimate \mathbf{K} . This is a compressed sensing problem for which many algorithms are

available. For the sake of decoder design, it is convenient to decouple the \mathbf{K} -estimation performance from the overall type estimation performance (3). Specifically, we use the average total variation distance between the empirical distributions induced by \mathbf{K} and $\widehat{\mathbf{K}}$ as the communication performance metric:

$$\overline{\mathbb{T}\mathbb{V}} = \mathbb{E} \left[\frac{1}{2} \sum_{i=1}^M \left| \frac{K_i}{\sum_{j=1}^M K_j} - \frac{\widehat{K}_i}{\sum_{j=1}^M \widehat{K}_j} \right| \right]. \quad (5)$$

Note that if $K_i \in \{0, 1\}, \forall i \in [M]$, $\overline{\mathbb{T}\mathbb{V}}$ coincides with the per-sensor error probability considered in UMA [1, Def. 1].

Let $p_{K_i}(k)$ be the marginal prior distribution of $K_i, i \in [M]$, obtained from the state distribution $p_{\mathcal{S}}$, the quantization mapping $q_{\mathcal{Q}}(\cdot)$, and the target selection distributions $\{p_{O_k}\}_{k=1}^{K_a}$. For example, if $p_{\mathcal{S}}$ and p_{O_k} are the uniform distributions over \mathcal{S} and $[M_a]$, respectively, and the quantization mapping preserves uniformity, we have that, for all $i \in [M]$,

$$p_{K_i}(k) = \sum_{m=0}^{M_a} \text{Bin} \left(m; M_a, \frac{1}{M} \right) \text{Bin} \left(k; K_a, \frac{m}{M_a} \right). \quad (6)$$

Indeed, the number of targets having a given quantized state index $i \in [M]$ follows a binomial distribution with parameters $(M_a, 1/M)$. Furthermore, given that this number is m , K_i follows a binomial distribution with parameters $(K_a, m/M)$.

A soft decoder computes the marginal posterior probability

$$p_{K_i | \mathbf{Y}}(k_i | \mathbf{y}) = \sum_{\{k_j\}_{j \neq i} \in \{0, 1, \dots, K_a\}^{M-1}} p_{\mathbf{K} | \mathbf{Y}}([k_1, \dots, k_M] | \mathbf{y}) \quad (7)$$

for $i \in [M]$, where $p_{\mathbf{K} | \mathbf{Y}}(\mathbf{k} | \mathbf{y}) = \frac{p_{\mathbf{Y} | \mathbf{K}}(\mathbf{y} | \mathbf{k}) p_{\mathbf{K}}(\mathbf{k})}{p_{\mathbf{Y}}(\mathbf{y})} \propto p_{\mathbf{Y} | \mathbf{K}}(\mathbf{y} | \mathbf{k}) p_{\mathbf{K}}(\mathbf{k})$ is the joint posterior probability of \mathbf{K} . The marginalization in (7) is cumbersome. Therefore, we seek to decouple (4) into M scalar Gaussian models of the form

$$R_i = K_i + \mathcal{N}(0, \xi_i), \quad i \in [M]. \quad (8)$$

As a result, given $R_i = r_i$, the marginal posterior mean and variance of K_i can be estimated by

$$\hat{k}_i = f(r_i, \xi_i) = \frac{\sum_{k=0}^{K_a} k p_{K_i}(k) \exp\left(-\frac{(r_i - k)^2}{2\xi_i}\right)}{\sum_{k=0}^{K_a} p_{K_i}(k) \exp\left(-\frac{(r_i - k)^2}{2\xi_i}\right)}, \quad (9)$$

$$\hat{v}_i = g(r_i, \xi_i) = \frac{\sum_{k=0}^{K_a} (k - \hat{k}_i)^2 p_{K_i}(k) \exp\left(-\frac{(r_i - k)^2}{2\xi_i}\right)}{\sum_{k=0}^{K_a} p_{K_i}(k) \exp\left(-\frac{(r_i - k)^2}{2\xi_i}\right)}, \quad (10)$$

respectively. The final estimate of \mathbf{K} is obtained by rounding $\widehat{\mathbf{k}} = [\hat{k}_1, \dots, \hat{k}_M]^T$ to the nearest integers. In the following, we present and compare three algorithms to obtain the scalar models that have been used in the literature [4], [9], [15].

A. Approximate Message Passing

We first consider the AMP estimator designed in [4, Sec. IV] for the UMA setting. At each iteration t , the following updates are performed:

$$\widehat{\mathbf{y}}^{(t)} = \mathbf{C}^T \mathbf{z}^{(t-1)} + \sqrt{NP} \widehat{\mathbf{k}}^{(t-1)}, \quad (11)$$

$$\widehat{\mathbf{k}}^{(t)} = f_i(\widehat{\mathbf{y}}^{(t)}), \quad (12)$$

$$\mathbf{z}^{(t)} = \mathbf{y} - \sqrt{\text{NPC}}\hat{\mathbf{k}}^{(t)} + \frac{M}{N}\mathbf{z}^{(t-1)}\langle f'_t(\hat{\mathbf{y}}^{(t)}) \rangle. \quad (13)$$

Here, $\langle \cdot \rangle$ denotes the arithmetic mean, and $f_t(\mathbf{r}) = [f(r_1, \xi^{(t-1)}), \dots, f(r_M, \xi^{(t-1)})]^T$ where $f(\cdot, \cdot)$ was defined in (9) and where $\xi^{(t-1)} = \|\mathbf{z}^{(t-1)}\|^2/N$. In (13), f'_t is the componentwise derivative of f_t . The estimate $\hat{\mathbf{k}}$ in the denoising step (12) is given by the posterior mean of $\{K_i\}_{i=1}^M$ obtained from the scalar models (8) with $\xi_i = \xi^{(t-1)}, \forall i \in [M]$, and the effective observation $[R_i, \dots, R_M]^T = \hat{\mathbf{y}}^{(t)}$.

The complexity of each iteration is of order $O(NM)$. It can be reduced to $O(\max\{M, N\} \log \max\{M, N\})$ if \mathbf{C} is a truncated Hadamard matrix, because $\mathbf{C}\hat{\mathbf{k}}^{(t)}$ and $\mathbf{C}^T\mathbf{z}^{(t-1)}$ can be computed efficiently using the Hadamard transform [4], [5].

B. Expectation Propagation

Next, we describe the EP algorithm developed in [15, Sec. IV-D]. We write the posterior probability $p_{\mathbf{K}|\mathbf{Y}}$ as

$$p_{\mathbf{K}|\mathbf{Y}}(\mathbf{k}|\mathbf{y}) \propto p_{\mathbf{Y}|\mathbf{K}}(\mathbf{y}|\mathbf{k})p_{\mathbf{K}}(\mathbf{k}) \quad (14)$$

$$\approx \mathcal{N}(\mathbf{y}; \sqrt{\text{NPC}}\mathbf{k}, \mathbf{I}_N) \prod_{i=1}^M p_{K_i}(k_i). \quad (15)$$

The approximation in (15) follows by ignoring the dependency between the $\{K_i\}_{i=1}^M$. Following EP, we write the posterior estimate in accordance with (15) as $\hat{p}_{\mathbf{K}|\mathbf{Y}}(\mathbf{k}|\mathbf{y}) = \hat{p}_0(\mathbf{k}) \prod_{i=1}^M \hat{p}_i(k_i)$, where $\hat{p}_0(\mathbf{k}) \propto \prod_{i=1}^M \mathcal{N}(k_i; \mu_{i0}, \xi_{i0})$ and $\hat{p}_i(k_i) \propto \mathcal{N}(k_i; \mu_{i1}, \xi_{i1})$. We iteratively update $\{\mu_{i0}, \xi_{i0}\}$, $\{\mu_{i1}, \xi_{i1}\}$, and the approximate posterior mean \hat{k}_i and variance \hat{v}_i . Specifically, at iteration t , $\hat{k}_i^{(t)} = f(\mu_{i0}^{(t)}, \xi_{i0}^{(t)})$ and $\hat{v}_i^{(t)} = g(\mu_{i0}^{(t)}, \xi_{i0}^{(t)})$. The terms $\{\mu_{i1}, \xi_{i1}\}$ are updated as

$$\xi_{i1}^{(t)} = (1/\hat{v}_i^{(t)} - 1/\xi_{i0}^{(t-1)})^{-1}, \quad (16)$$

$$\mu_{i1}^{(t)} = \xi_{i1}^{(t)}(\hat{k}_i^{(t)}/\hat{v}_i^{(t)} - \mu_{i0}^{(t-1)}/\xi_{i0}^{(t-1)}). \quad (17)$$

Furthermore, the terms $\{\mu_{i0}, \xi_{i0}\}$ are updated as

$$\xi_{i0}^{(t)} = (1/\hat{\xi}_{i0} - 1/\xi_{i1}^{(t)})^{-1}, \quad (18)$$

$$\mu_{i0}^{(t)} = \xi_{i0}^{(t)}(\hat{\mu}_{i0}/\hat{\xi}_{i0} - \mu_{i1}^{(t)}/\xi_{i1}^{(t)}). \quad (19)$$

Here, $\hat{\xi}_{i0}$ is the i th diagonal element of the matrix

$$\hat{\Xi}_0 = \Xi_1 - \Xi_1\mathbf{C}^T((\text{NP})^{-1}\mathbf{I}_N + \mathbf{C}\Xi_1\mathbf{C}^T)^{-1}\mathbf{C}\Xi_1 \quad (20)$$

and $\hat{\mu}_{i0}$ is the i th element of

$$\hat{\boldsymbol{\mu}}_0 = \hat{\Xi}_0(\Xi_1^{-1}\boldsymbol{\mu}_1 + \sqrt{\text{NPC}}^T\mathbf{y}) \quad (21)$$

with $\boldsymbol{\mu}_1 = [\mu_{11}^{(t)}, \mu_{21}^{(t)}, \dots, \mu_{M1}^{(t)}]^T$ and $\Xi_1 = \text{diag}(\xi_{11}^{(t)}, \xi_{21}^{(t)}, \dots, \xi_{M1}^{(t)})$. The complexity of each iteration is of order $O(\min\{M, N\}^2 \max\{M, N\})$, and is dominated by the computation of $\hat{\Xi}_0$ in (20).

C. Scalar AMP

Finally, we consider the scalar AMP algorithm derived in [15, Sec. IV-C] and adopted in [9] for a type-based estimation problem associated to federated learning. Note that this algorithm was derived as a simplification of EP rather than of the AMP algorithm in Section III-A. In each iteration t , the approximate posterior mean $\hat{k}_i^{(t)}$ and variance $\hat{v}_i^{(t)}$ of K_i

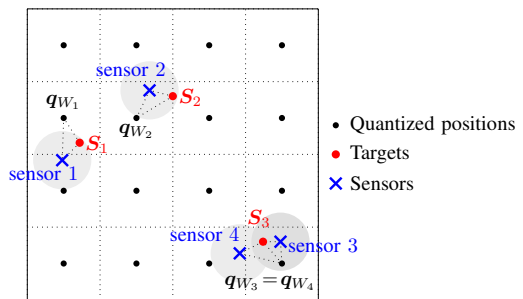


Fig. 2. An example of multi-target position tracking in a square with $M_a = 3$ targets, $K_a = 4$ sensors, and $M = 16$ quantized positions.

are given by $f(r_i^{(t)}, \xi_i^{(t)})$ and $g(r_i^{(t)}, \xi_i^{(t)})$, respectively. Here, the effective observation r_i and effective noise variance ξ_i , $i \in [M]$, are updated as

$$\xi_i^{(t)} = \left(\sum_{j=1}^N \frac{c_{ji}^2}{(\text{NP})^{-1} + v_j^{(t)}} \right)^{-1}, \quad (22)$$

$$r_i^{(t)} = \hat{k}_i^{(t)} + \xi_i^{(t)} \sum_{j=1}^N \frac{c_{ji}(y_j/\sqrt{\text{NP}} - z_j^{(t)})}{(\text{NP})^{-1} + v_j^{(t)}}, \quad (23)$$

where c_{ji} is the (j, i) th entry of \mathbf{C} . Furthermore, v_j and z_j , $j \in [N]$, are updated as

$$v_j^{(t)} = \sum_{i=1}^M c_{ji}^2 \hat{v}_i^{(t)}, \quad z_j^{(t)} = \sum_{i=1}^M c_{ji} \hat{k}_i^{(t)} - v_j^{(t)} \frac{y_j/\sqrt{\text{NP}} - z_j^{(t-1)}}{(\text{NP})^{-1} + v_j^{(t-1)}}.$$

The complexity of each iteration is of order $O(NM)$.

To summarize, AMP has a lower complexity than EP, and if a truncated-Hadamard codebook is used, it also has a lower complexity than scalar AMP.

IV. MULTI-TARGET POSITION TRACKING

We consider a scenario where K_a sensors track the position of M_a targets placed uniformly at random in a square area \mathcal{S} of size 1×1 . The area is divided into a regular grid consisting of M disjoint cells whose centroids form the set of quantized positions \mathcal{Q} . Each sensor tracks a target chosen uniformly at random from the M_a targets.³ Sensor k determines the position of its target, maps this position to the closest quantized position indexed by W_k , and sends the codeword c_{W_k} to the receiver. In Fig. 2, we illustrate an example with $M_a = 3$ targets, $K_a = 4$ sensors, and $M = 16$ quantized positions.

We generate \mathbf{C} as a truncated Hadamard matrix. We assume that the receiver uses the AMP, scalar AMP, or EP decoder described in Section III, with the prior given in (6).⁴ We set the maximum number of iterations to 10, and terminate the iterations early if the estimate of \mathbf{K} remains unchanged after an iteration. We first compare the ability of these decoders to recover \mathbf{K} by evaluating the average total variation distance

³More practical sensor deployment and target selection will be considered in future works.

⁴This requires that the receiver knows both K_a and M_a . Our decoder can be extended to the case of unknown K_a and M_a . In this case, we initialize these parameters and refine their values, and also the prior, along the iterations.

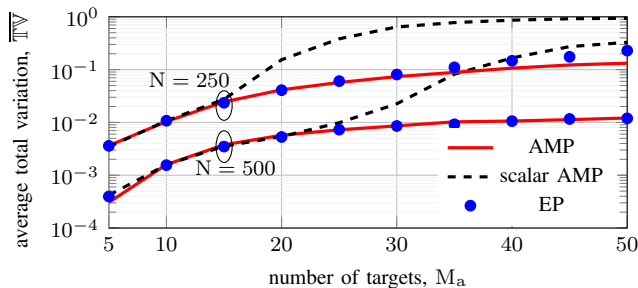


Fig. 3. The average total variation $\overline{\mathbb{T}\mathbb{V}}$ vs. the number of targets M_a for $K_a = 50$ sensors, $\log_2 M = 10$ bits, and the SNR $P = -12$ dB.

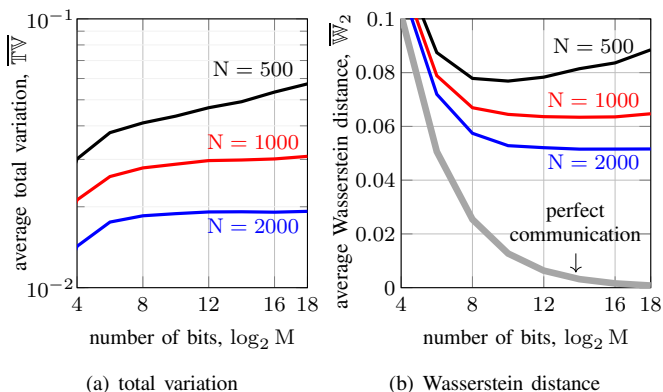


Fig. 4. The average total variation $\overline{\mathbb{T}\mathbb{V}}$ and average 2-Wasserstein distance $\overline{\mathbb{W}}_2$ vs. the number of bits $\log_2 M$ for $K_a = 100$ sensors, $M_a = 10$ targets, and the SNR $P = -27$ dB.

$\overline{\mathbb{T}\mathbb{V}}$ in (5). In Fig. 3, we plot $\overline{\mathbb{T}\mathbb{V}}$ for the three decoders as a function of the number of targets M_a for a setting with $N \in \{250, 500\}$ channel uses, $K_a = 50$ sensors, $\log_2 M = 10$ bits, and the SNR $P = -12$ dB. For small M_a values, the three decoders perform similarly. However, as M_a increases, AMP outperforms both EP and scalar AMP, which exhibits the worst performance. Overall, AMP is preferable because of both complexity and performance advantages.

Next, we investigate the impact of the quantization resolution, represented by the number of bits $\log_2 M$. In Fig. 4, we plot both $\overline{\mathbb{T}\mathbb{V}}$ and the average Wasserstein distance $\overline{\mathbb{W}}_2$ achieved with AMP as functions of $\log_2 M$ for $N \in \{500, 1000, 2000\}$ channel uses, $K_a = 100$ sensors, $M_a = 10$ targets, and the SNR $P = -27$ dB. We also show the value of $\overline{\mathbb{W}}_2$ achieved if there is no communication error (i.e., if $\widehat{\mathbf{K}} = \mathbf{K}$), which accounts only for the quantization distortion. As the quantization resolution increases, this distortion decreases. However, increasing M for a fixed N leads to a higher transmission rate, and a consequent degradation of the communication performance, as shown by the increase of $\overline{\mathbb{T}\mathbb{V}}$ observed in Fig. 4(a). Due to this tradeoff, the average Wasserstein distance is minimized at an intermediate value of M , as observed in Fig. 4(b). The optimal value of M exceeds N , indicating that the use of an orthogonal codebook, as in TBMA, is suboptimal. As N grows, the $\overline{\mathbb{W}}_2$ curve flattens out around its minimum.

For the considered coding scheme, N and M cannot be increased beyond the values chosen in Fig. 4 because of complexity. To address the case $\log_2 M \gg 18$, one needs to

use coded-compressed sensing solutions as in [4], [5].

V. CONCLUSIONS

We formulated TUMA: a framework in which a large number of users track the state of multiple processes. Each user quantizes the state of its tracked process and sends, in an uncoordinated manner, the quantization index to the receiver, which then estimates the type of the quantized states. We used the Wasserstein distance to evaluate the type estimation error. Our results showcased the effectiveness of AMP for accurate type estimation. Furthermore, we identified a trade-off between quantization resolution and communication error when minimizing the Wasserstein distance.

REFERENCES

- [1] Y. Polyanskiy, "A perspective on massive random-access," in *Proc. IEEE Int. Symp. Inf. Theory (ISIT)*, Aachen, Germany, Jun. 2017, pp. 2523–2527.
- [2] S. S. Kowshik, K. Andreev, A. Frolov, and Y. Polyanskiy, "Energy efficient coded random access for the wireless uplink," *IEEE Trans. Commun.*, vol. 68, no. 8, pp. 4694–4708, Jun. 2020.
- [3] K.-H. Ngo, A. Lancho, G. Durisi, and A. Graell i Amat, "Unsourced multiple access with random user activity," *IEEE Trans. Inf. Theory*, vol. 69, no. 7, pp. 4537–4558, Jul. 2023.
- [4] A. Fengler, P. Jung, and G. Caire, "SPARCs for unsourced random access," *IEEE Trans. Inf. Theory*, vol. 67, no. 10, pp. 6894–6915, Oct. 2021.
- [5] V. K. Amalladinne, A. K. Pradhan, C. Rush, J.-F. Chamberland, and K. R. Narayanan, "Unsourced random access with coded compressed sensing: Integrating AMP and belief propagation," *IEEE Trans. Inf. Theory*, vol. 68, no. 4, pp. 2384–2409, Apr. 2022.
- [6] J. Hoffman and R. Mahler, "Multitarget miss distance via optimal assignment," *IEEE Trans. Syst. Man. Cybern. A Syst. Human.*, vol. 34, no. 3, pp. 327–336, May 2004.
- [7] D. Schuhmacher, B.-T. Vo, and B.-N. Vo, "A consistent metric for performance evaluation of multi-object filters," *IEEE Trans. Signal Process.*, vol. 56, no. 8, pp. 3447–3457, Aug. 2008.
- [8] A. S. Rahmthullah, A. F. Garcia-Fernández, and L. Svensson, "Generalized optimal sub-pattern assignment metric," in *Proc. Int. Conf. Inf. Fus. (FUSION)*, Xi'an, China, 2017, pp. 1–8.
- [9] L. Qiao, Z. Gao, Z. Li, and D. Gündüz, "Unsourced massive access-based digital over-the-air computation for efficient federated edge learning," in *Proc. IEEE Int. Symp. Inf. Theory (ISIT)*, Taipei, Taiwan, Jun. 2023.
- [10] D. Gündüz, F. Chiariotti, K. Huang, A. E. Kalør, S. Kobus, and P. Popovski, "Timely and massive communication in 6G: Pragmatics, learning, and inference," *IEEE BITS Inf. Theory Mag.*, vol. 3, no. 1, pp. 27–40, Mar. 2023.
- [11] G. Mergen and L. Tong, "Type based estimation over multiaccess channels," *IEEE Trans. Signal Process.*, vol. 54, no. 2, pp. 613–626, 2006.
- [12] J. Dommel, Z. Utkovski, O. Simeone, and S. I. Stańczak, "Joint source-channel coding for semantics-aware grant-free radio access in IoT fog networks," *IEEE Signal Process. Lett.*, vol. 28, pp. 728–732, Apr. 2021.
- [13] M. Zhu, C. Feng, C. Guo, N. Jiang, and O. Simeone, "Information bottleneck-inspired type based multiple access for remote estimation in IoT systems," *IEEE Signal Process. Lett.*, vol. 30, pp. 403–407, Apr. 2023.
- [14] G. Peyré and M. Cuturi, "Computational optimal transport: With applications to data science," *Foundations and Trends® in Machine Learning*, vol. 11, no. 5-6, pp. 355–607, Feb. 2019.
- [15] X. Meng, L. Zhang, C. Wang, L. Wang, Y. Wu, Y. Chen, and W. Wang, "Advanced NOMA receivers from a unified variational inference perspective," *IEEE J. Select. Areas Commun.*, vol. 39, no. 4, pp. 934–948, Apr. 2021.
- [16] I. Zadik, Y. Polyanskiy, and C. Thrampoulidis, "Improved bounds on Gaussian MAC and sparse regression via Gaussian inequalities," in *Proc. IEEE Int. Symp. Inf. Theory (ISIT)*, Paris, France, Jul. 2019, pp. 430–434.

- [17] K.-H. Ngo, G. Durisi, A. Graell i Amat, P. Popovski, A. E. Kalør, and B. Soret, "Unsourced multiple access with common alarm messages: Network slicing for massive and critical IoT," *IEEE Trans. Commun.*, vol. 72, no. 2, pp. 907–923, Feb. 2024.
- [18] C. Bian, Y. Shao, and D. Gündüz, "Wireless point cloud transmission," *arXiv preprint arXiv:2306.08730*, 2023.

This figure "fig1.png" is available in "png" format from:

<http://arxiv.org/ps/2404.19552v1>